Chapter

Design, Synthesis, and Biological Applications of Boron-Containing Polyamine and Sugar Derivatives

Shin Aoki, Hiroki Ueda, Tomohiro Tanaka, Taiki Itoh, Minoru Suzuki and Yoshinori Sakurai

Abstract

Boron (B), an element that is present in ultratrace amounts in animal cells and tissues, is expected to be useful in many scientific fields. We have found the hydrolysis of C–B bond in phenylboronic acid-pendant cyclen (cyclen = 1,4,7,10-tetraazacyclododecane) and the full decomposition of *ortho*-carborane attached with cyclen and ethylenediamines in aqueous solution at neutral pH upon complexation with intracellular metals. The change in the chemical shift of the ^{11}B signals in ^{11}B-NMR spectra of these boron-containing metal chelators can be applied to the magnetic resonance imaging (MRI) of metal ions in solutions and in living cells. More important applications of B would be boron neutron capture therapy (BNCT) based on the nuclear reaction between ^{10}B atoms and thermal neutrons, yielding $^{4}He^{2+}$ (α) and $^{7}Li^{3+}$ ions, which destroy ^{10}B-containing cancer cells. The design and synthesis of new BNCT agents based on sugars and macrocyclic polyamines and their Zn^{2+} complexes are also introduced in this review.

Keywords: boron-10 (^{10}B), boron-11 (^{11}B), magnetic resonance imaging, metal probes, decomposition reactions, carborane, boron neutron capture therapy, macrocyclic polyamines, sugars

1. Introduction

Boron (B) is an element that is found in ultratrace amounts in mammalian cells and consists of two stable isotopes, boron-10 (^{10}B) and boron-11 (^{11}B), with a natural abundance ratio ($^{10}B/^{11}B$ = 19.9/80.1). The most important properties of boron compounds with respect to biological and medical sciences would be: (1) ^{11}B atoms have a higher NMR sensitivity (16.5% for ^{11}B and 2.0% for ^{10}B relative to ^{1}H NMR), thus permitting the detection of B-containing drugs themselves and analytes that react with B-containing probes in living systems [1]; and (2) the ^{10}B nucleus possesses a high reactivity with thermal neutrons resulting in the generation of two radioactive species (^{4}He and ^{7}Li particles), which induce the excitation and ionization of molecules within short path lengths [2]. For the above reasons, boron compounds can be useful in biological applications for the treatment and diagnosis of cancer and other diseases [3].

In 1936, Locher proposed the concept of boron neutron capture therapy (BNCT) based on the aforementioned nuclear reaction between ^{10}B and thermal neutrons [4]. Because the destructive effect of the two heavy particles (^{4}He and ^{7}Li particles) that are generated by the decomposition of ^{10}B lies within 5–9 μm, which is close to the size of living cells, single-cell treatment would be possible by the achievement of cancer-specific delivery of ^{10}B and irradiation with a sufficient intensity of thermal neutrons [5–7].

BNCT systems have been installed in clinical facilities as a method for the noninvasive treatment of certain types of cancers such as recurrent head and neck cancer and malignant gliomas [8]. The selective and efficient accumulation of boron into tumor tissues is one of the important clues for successful BNCT and, as described below, two boron compounds have been approved for use as BNCT drugs. In addition, monitoring the distribution of boron in patients is required for planning treatment protocols to determine the irradiation doses and positions of the patient [9].

In this review, we introduce the applications of boron compounds to ^{11}B NMR (nuclear magnetic resonance)/MRI (magnetic resonance imaging) probes for the sensing of intracellular metal ions and BNCT agents for use in the treatment of cancer. The d-block metal ion probes take advantage of changes in the chemical shift in ^{11}B NMR spectra due to the cleavage of the carbon-boron bond in phenylboronic acid-pendant cyclen (1,4,7,10-tetraazacyclododecane) and the decomposition of the *ortho*-carborane moieties of carborane-metal chelator hybrids upon complexation with metal ions in aqueous solution at neutral pH. In the second half of this review, the development of novel BNCT agents bearing sugar and macrocyclic polyamine scaffolds is described.

2. ^{11}B NMR and MRI probes for metal ions in solutions and in living cells based on carbon-boron bond cleavage and the decomposition of *ortho*-carboranes upon metal complexation of chelator units

2.1 General

Biologically essential d-block metal ions such as zinc (Zn^{2+}), copper (Cu^{2+}), manganese (Mn^{2+}), and iron (Fe^{2+}) are involved in a variety of physiological processes in living systems as cofactors for various enzymes, intracellular second messengers, and related processes [10]. It was reported that a metal imbalance in cells and tissues causes a number of disorders such as Alzheimer's disease, Parkinson's disease, Willson's disease, etc. [10]. Therefore, the development of fluorescence-based probes for the detection of these intracellular metal ions has contributed to our understanding of their functions and metabolism in living cells, while some limitations to detecting their emission from tissues remain due to their impermeability [10–12].

It is well known that MRI is one of the useful noninvasive methods for *in vivo* visualization and that it permits three-dimensional images of organisms and drug distributions to be obtained [13]. Although MRI is powerful method, there are only a few examples of MRI probes such as Gd^{3+}-based contrast agents [14, 15].

2.2 Development of d-block metal ions probes based on the cleavage of C–B bonds in B-containing probes

It is well established that macrocyclic polyamine ligands such as 1,4,7-triazacyclononane ([9]aneN_3) **1**, 1,4,7,10-tetraazacyclododecane ([12]aneN_4, cyclen) **2**, and

1,4,7,10,13-pentaazacyclopentadecane ([15]aneN$_5$) **3** are able to form more stable complexes **4**–**6** with metal ions such as Cu^{2+}, Ni^{2+}, and Zn^{2+} in aqueous solution (**Figure 1**) than metal complexes of linear polyamine types [16, 17]. In addition, metal ions in these complexes, especially the Zn^{2+} ion in Zn^{2+}-cyclen complex (**5**), possess strong Lewis acidity and the deprotonated Zn^{2+}-bound H_2O (HO^-) functions as a nucleophile and a base in aqueous solution at neutral pH [18–23].

Bendel and coworkers reported that ^{11}B NMR/MRI would be a potential technique for the imaging of boron agents in the body [24, 25]. However, a functional system for achieving this has not been established yet. In this context, we hypothesized that the sp^2 boron in **7** and **8** would be changed to the sp^3 boron due to the formation of metal complexes **9a** and **10a** and the following interaction of metal-bound H_2O (OH^-) with boron at neutral pH, resulting in change in the ^{11}B NMR signals (**Figure 2**) [26]. However, the products obtained after the addition of Zn^{2+} to **7** (L^1) (**Figure 3a**) were **11a** (ZnL^3) and boric acid ($B(OH)_3$), as confirmed by an X-ray structure analysis (**Figure 3b**). The findings strongly indicated that the Zn^{2+}-bound H_2O (**9a** and **10a**) is efficiently deprotonated

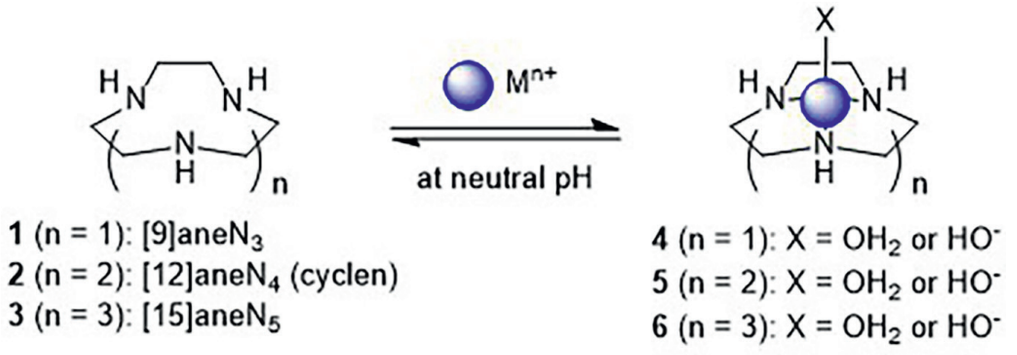

Figure 1.
The structures of 9-, 12-, and 15-membered macrocyclic polyamines **1**–**3** *and their metal complexes* **4**–**6**.

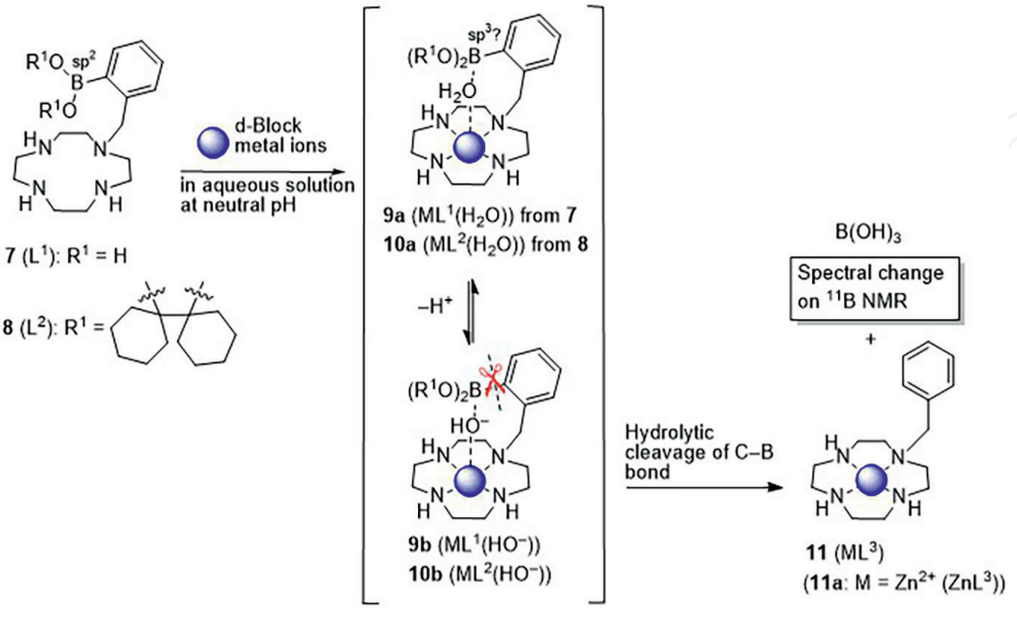

Figure 2.
The C–B bond hydrolysis of phenylboronic acid-pendant 12-membered tetraamine (cyclen) to produce inorganic boric acid.

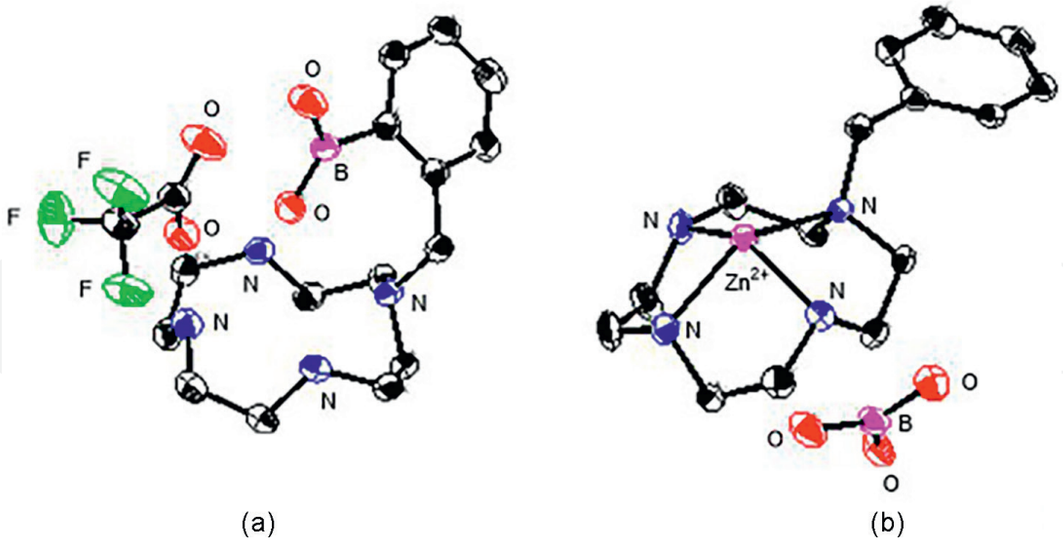

Figure 3.
X-ray crystal structures of (a) **7** *(L^1) and (b)* **11a** *(ZnL^3) with $B(OH)_3$.*

due to the double activation by Zn^{2+} and B to produce the Zn^{2+}-bound HO^- (**9b** and **10b**), which hydrolyzes the C–B bond. The hydrolytic cleavage of the C–B bond of **7** (L^1) was also observed by the measurement of ^{11}B NMR upon the addition of Zn^{2+}, in which the ^{11}B NMR signal of **7** (L^1) at 31.1 ppm was shifted to 19.4 ppm that corresponds to $B(OH)_3$.

The ^{11}B NMR spectral change of **7** (L^1) was promoted by Cu^{2+}, Fe^{2+}, Co^{2+}, and Ni^{2+} but not by Ca^{2+} and Mg^{2+} (**Table 1**). Hydrolysis of the C–B bond of **7** (L^1) with Cd^{2+} was faster than that with Zn^{2+}, possibly due to the strong nucleophilicity of the Cd^{2+}-bound HO^- [27]. Meanwhile, the C–B bond cleavage of **7** (L^1) by Mn^{2+} and Fe^{3+} was slow.

The intracellular uptake of boron in **7** and **8** into Jurkat T cells was determined by ICP-AES, and the results indicated that the uptake of **8** was higher than that of **7**, possibly due to the hydrophobicity of the boronic ester group. The Zn^{2+}-induced C–B bond cleavage of **8** (L^2) by intracellular Zn^{2+} was observed in living cells. The Jurkat T cells were sequentially treated with **8** (L^2) and Zn^{2+} complex of pyrithione (Zn^{2+} ionophore to transfer Zn^{2+} into cells) for 20 min and 1 h, respectively. The cells were washed with CS-RPMI and PBS and then transferred to a quartz NMR tube, whose

	δ (ppm)	Δδ (ppm)[b]	time (h)[c]		δ (ppm)	Δδ (ppm)[b]	time (h)[c]
7 (L^1) alone	31.1	–	–	Mn^{2+}	20.6	–10.5	48
Zn^{2+}	19.4	–11.7	0.5	Ni^{2+}	19.8	–11.3	2
Cu^{2+}	19.5	–11.6	1.5	Cd^{2+}	19.2	–11.9	0.1
Fe^{2+}	19.7	–11.6	0.5	Ca^{2+}	31.7	0.6	–
Fe^{3+}	30.8	–0.3	–	Mg^{2+}	31.9	0.8	–
Co^{2+}	19.6	–11.5	1				

[a] *All data are referenced to external $BF_3{\cdot}Et_2O$ in $CDCl_3$ (δ = 0 ppm).*
[b] *Δδ = δ (**7** (L^1) with metal ions) – δ (**7** (L^1)).*
[c] *Approximate reaction time for the completion of C–B bond cleavage.*

Table 1.
*^{11}B NMR spectral change of **7** (L^1) (20 mM) upon the addition of d-block metal ions (20 mM) in 1 M HEPES buffer at pD 7.4 and 25 °C [26].*[a]

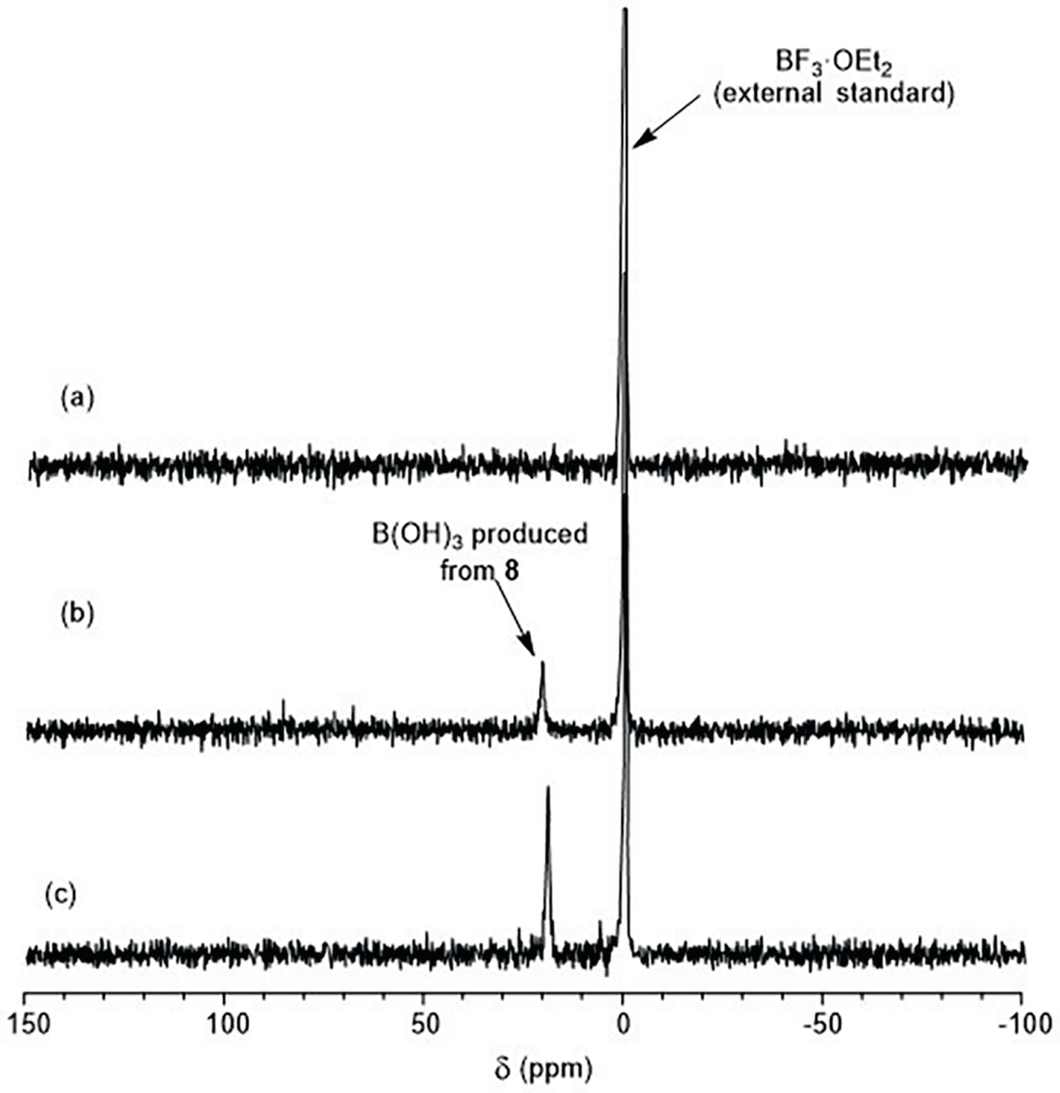

Figure 4.
In-cell ^{11}B NMR spectra of **8** *(L^2) in the absence of Zn^{2+}–pyrithione (ionophore) and in the presence of Zn^{2+}–pyrithione ($BF_3{\cdot}Et_2O$ was used as an external references). The Jurkat T cells (4×10^8 cells) were incubated with 33 μM* **8** *(L^2) in culture medium at 37 °C for 1 h, and then (a) DMSO (as negative control), (b) 2.5 μM Zn^{2+}–pyrithione, and (c) 10 μM Zn^{2+}–pyrithione at 37 °C for 20 min.*

^{11}B NMR spectra were measured in D_2O containing PBS. As shown in **Figure 4**, the ^{11}B signal for $B(OH)_3$ (ca. 19 ppm) in Jurkat T cells was observed with a positive correlation to the concentrations of Zn^{2+}-pyrithione complex, indicating the successful detection of the intracellular Zn^{2+} ions. It should be noted that the ^{11}B signal for **8** (ca. 31 ppm) in the absence of Zn^{2+} was observed as a broad signal.

2.3 Development of Cu^{2+} ion probes based on decomposition reaction of *ortho*-carborane–metal chelator hybrids

It is known that the reaction of the *o*-carborane **12** with Brønsted or Lewis bases affords the corresponding *nido*-form **13** and $B(OH)_3$ and that the further degradation of **13** proceeds slowly under harsh conditions such as in acidic solutions and/or at high temperatures (**Figure 5**) [28]. On the other hand, we found that *o*-carborane derivatives such as **12**, **14**, and **15a–c** generate 4–9 equiv. of $B(OH)_3$ upon the reaction with

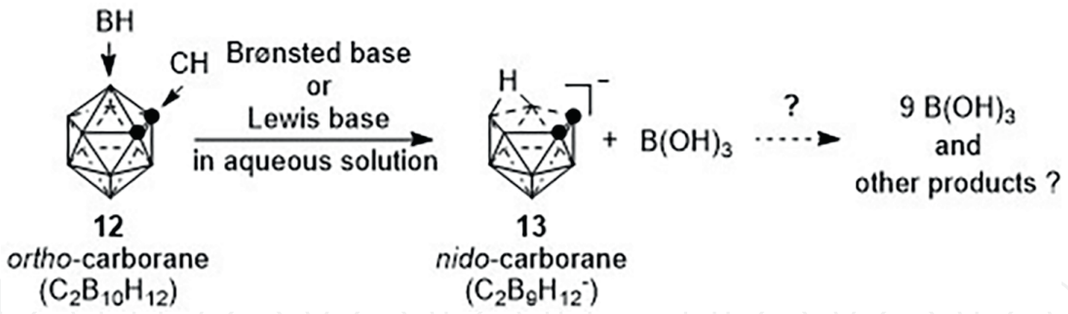

Figure 5.
Decomposition of o-carborane **12** *in the presence of a Brønsted or Lewis base.*

Cu^{2+} and Mn^{2+} via the corresponding *nido*-forms **12'**, **14'**, and **15a'–c'** under physiological conditions (**Figure 6a**) [29]. Our studies also indicated that the modification of *nido-o*-carborane (**16** (L^5)) with *N*,*N*,*N'*-trimethylethylenediamine (TriMEDA) as

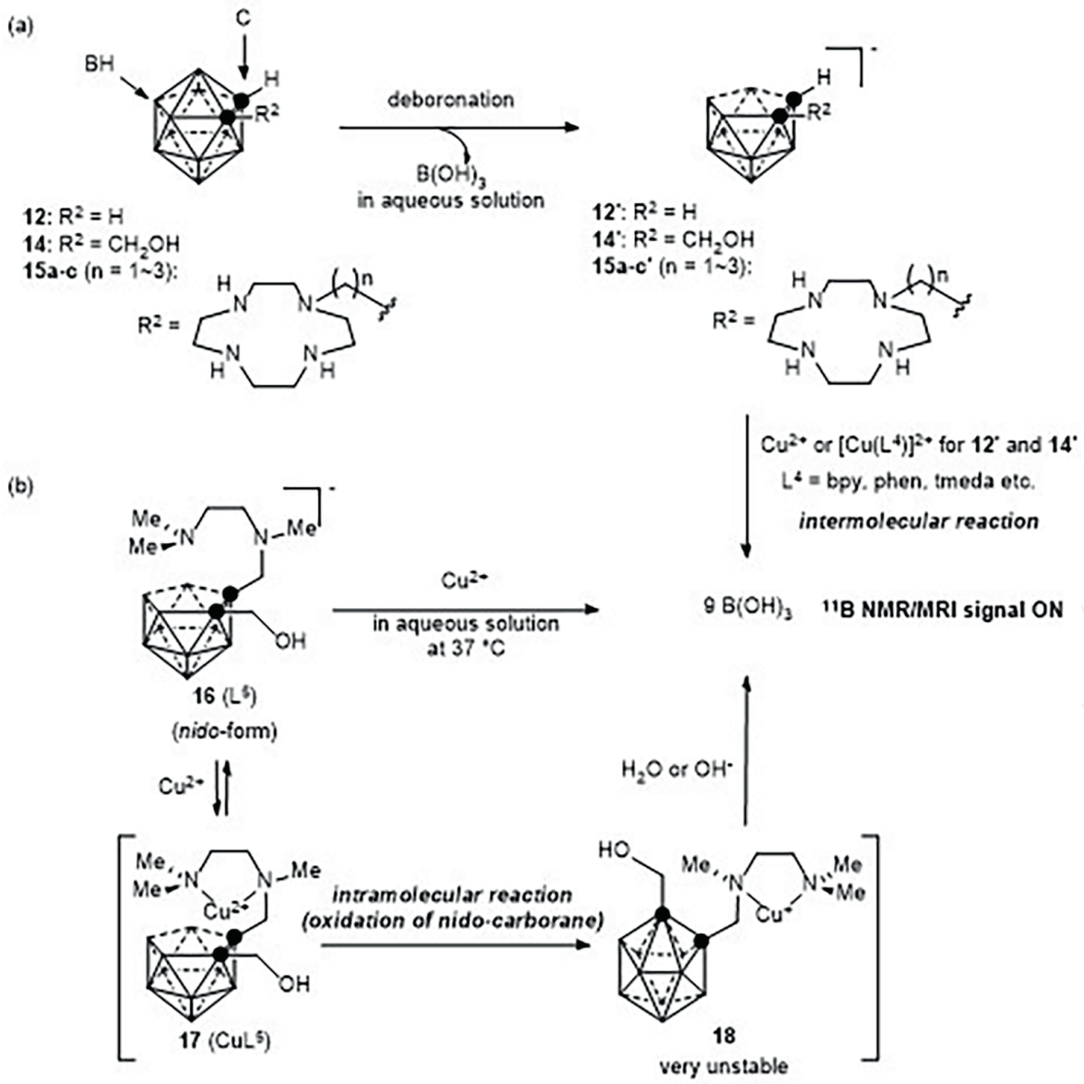

Figure 6.
Decomposition of o-carborane-pendant chelators (a) the ^{11}B *NMR/MRI detection of* Cu^{2+} *ion based on decomposition reaction of o-carborane derivatives and (b).*

a chelator unit facilitates the Cu-promoted decomposition of the molecule (**Figure 6b**) via the Cu^{2+}-complex **17** (CuL^5) to produce 9 $B(OH)_3$ in aqueous solution [30].

Changes in the ^{11}B NMR spectra of **16** (L^5) in the presence of various d-block metal ions are shown in **Figure 7**. A strong ^{11}B signal at ca. 20 ppm corresponding to $B(OH)_3$ was observed in the presence of Cu^{2+}, while, in the presence of other metal ions, the change was negligible. These results showed good agreement with the results of an azomethine-H assay, which also indicate the Cu^{2+} selectivity.

As shown in **Figure 8**, the oxidation potentials of **12′**, **14′**, and **16** are +0.57, +0.51, and +0.38 V (vs Ag/AgCl), respectively (determined by cyclic voltammetry), which are less positive than +0.7 V (vs Ag/AgCl) for $[Cu(TMEDA)]^+/[Cu(TMEDA)]^{2+}$. These data may explain the reasons why **12′**, **14′**, and **16** are oxidized by $Cu(TMEDA)]^{2+}$ complex. More efficient oxidation of **16** by Cu^{2+} than that of **12′** and **14′** is possibly due to the order of oxidation potentials (+0.38 V for **16** vs +0.57 and +0.51 V for **12′** and **14′**) and the close contact between the *o*-carborane unit and stable Cu^{2+}-TMEDA complex part in **17** and **18** (**Figure 6**).

In addition, the chemical yields of $B(OH)_3$ from **16** (L^5) with Cu^+ were decreased when antioxidants (sodium ascorbate, NaAsc) were added to the reaction mixture. According to these results and DFT calculations, a proposed mechanism for the decomposition of *o*-carborane moieties by Cu^{2+} is shown in **Figure 9**. Initially, the *nido*-form **20** is generated from the *closo*-form **19** by reaction with a nucleophile such

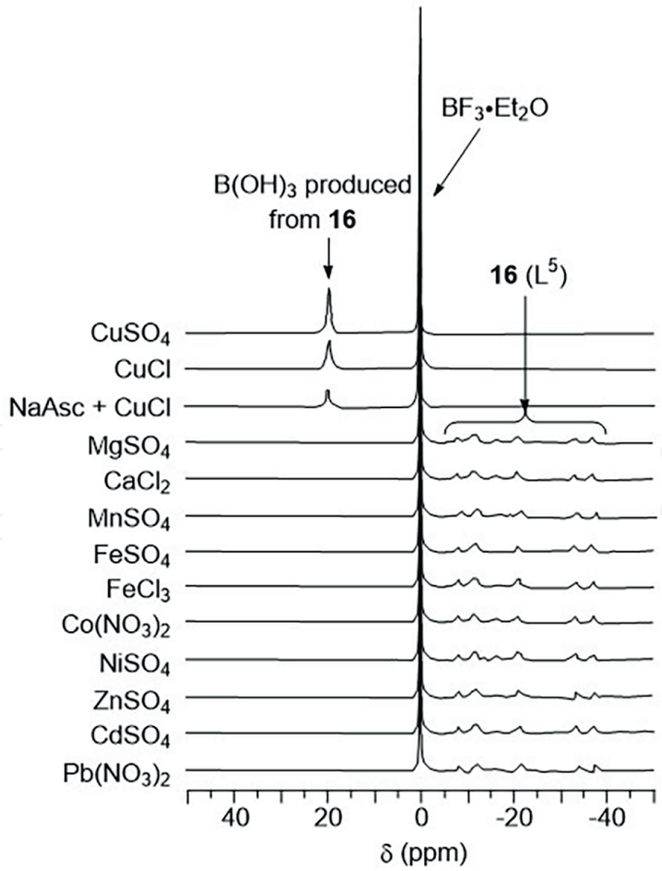

Figure 7.
Decomposition of **16** *(L^5) (1.4 mM) in the presence of Cu^{2+}, Cu^+, Cu^++NaAsc, Mg^{2+}, Ca^{2+}, Mn^{2+}, Fe^{2+}, Fe^{3+}, Co^{2+}, Ni^{2+}, Zn^{2+}, Cd^{2+} and Pb^{2+} (2 mM) in DMSO/0.5 M HEPES buffer (pH 7)/D_2O (5:4:1, 0.5 mL in total) at 37 °C after incubation for 4 h measured by $^{11}B\{^1H\}$ NMR. For $^{11}B\{^1H\}$ NMR experiments, 2.5% $BF_3{\cdot}Et_2O$ in $CDCl_3$ was used for an external reference.*

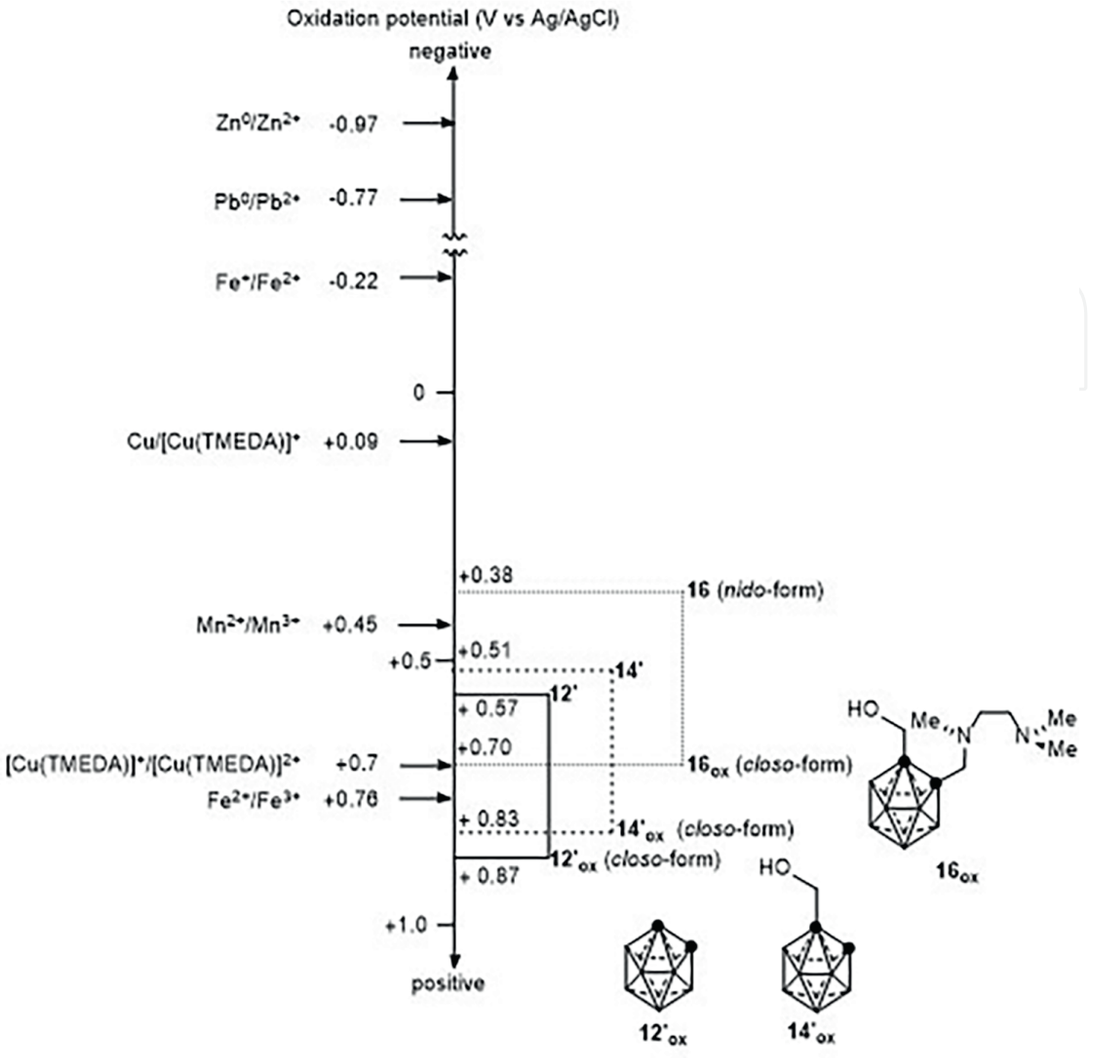

Figure 8.
Summary of the oxidation potentials of **12′**, **14′**, *and* **16** *(nido-form) with redox potentials of Cu, Fe, Pb, and Zn.*

as HO^-. Following the oxidation of the electronegative B10 (B at the 10 position) of **20** by Cu^{2+}, the *closo*-form **21** is produced by a ring-closure reaction. The unstable intermediate **21** would react with H_2O at the B9 position and is then completely decomposed to 9 equiv. of $B(OH)_3$ and other products via the transition state **22**.

^{11}B MRI experiments were conducted by using an aqueous solution of $B(OH)_3$ (10 mM) and Cu(bpy) (1 mM) in a larger vial (S_{out}) and a *o*-carborane analogue **14** (**Figure 6**) (1 mM) in a smaller vial (S_{in}) that was nested in the larger vial (**Figure 10**). To detect these boron compounds separately, BF1 (the basic transmitter frequency) values for $B(OH)_3$ and **14** are set ca. 128.392 and 128.387 MHz, respectively, because they have different chemical shifts (a-i and b-i in **Figure 10**). Besides, ^{11}B NMR images are obtained by using a two-dimensional ultra-short echo time sequence (UTE2D) with TE (echo time) of 199 μsec and TR (repetition time) of 30 msec. The ^{11}B signals for both $B(OH)_3$ and the *o*-carborane derivatives **14** were clearly observed, as shown in **Figure 10** (a-ii and b-ii).

The detection of Cu^{2+} by a ^{11}B NMR probe **16** (L^5) (2 mM) was carried out by the measurement of ^{11}B MRI and NMR at the increasing concentrations of Cu^{2+} (0, 0.02, 0.1, 0.2, 1.0, and 2.0 mM) in aqueous solution at neutral pH. The ^{11}B MRI/

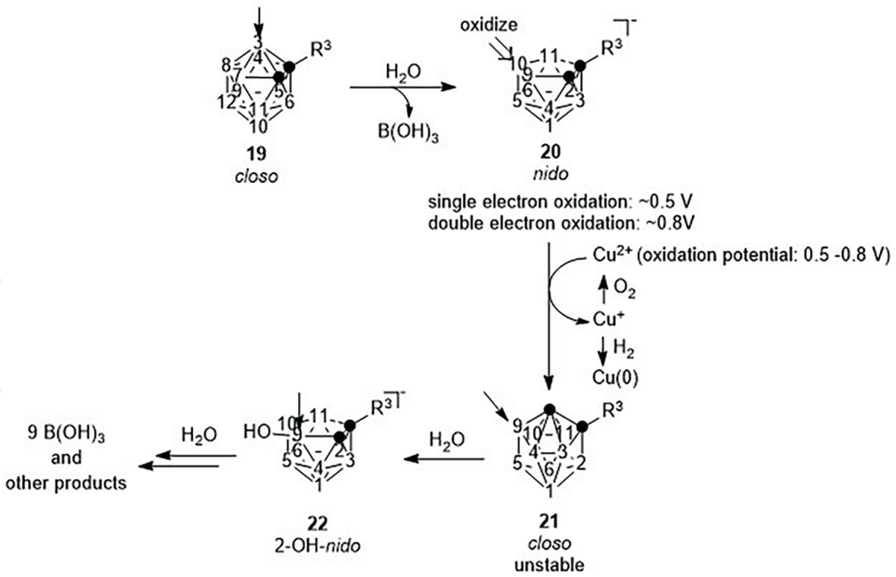

Figure 9.
Proposed mechanism for the decomposition reaction (arrows indicate positively charged boron atoms, which are susceptible to attack by H_2O or HO^-).

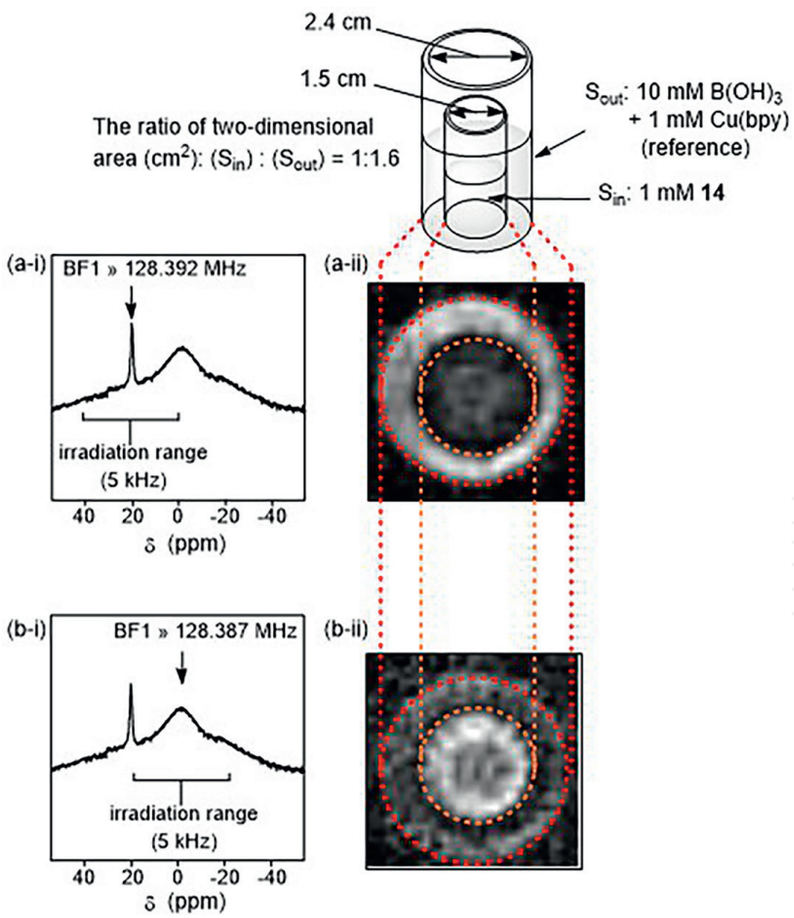

Figure 10.
*^{11}B MRI images differentiating $B(OH)_3$ and **14**. Curves (a-i) and (b-i) show typical ^{11}B NMR spectra of solutions in two vials (inside vial contains 1 mM **14** and outside contains 10 mM $B(OH)_3$). Images (a-ii) and (b-ii) show ^{11}B MRI of the inside vial (S_{in}) containing 1 mM **14** and the outside vial (S_{out}) including 10 mM $B(OH)_3$ + 1 mM Cu(bpy). Both ^{11}B NMR images were acquired by a two dimensional ultra-short echo time sequence (UTE2D) with TE = 199 μsec and TR = 30 msec.*

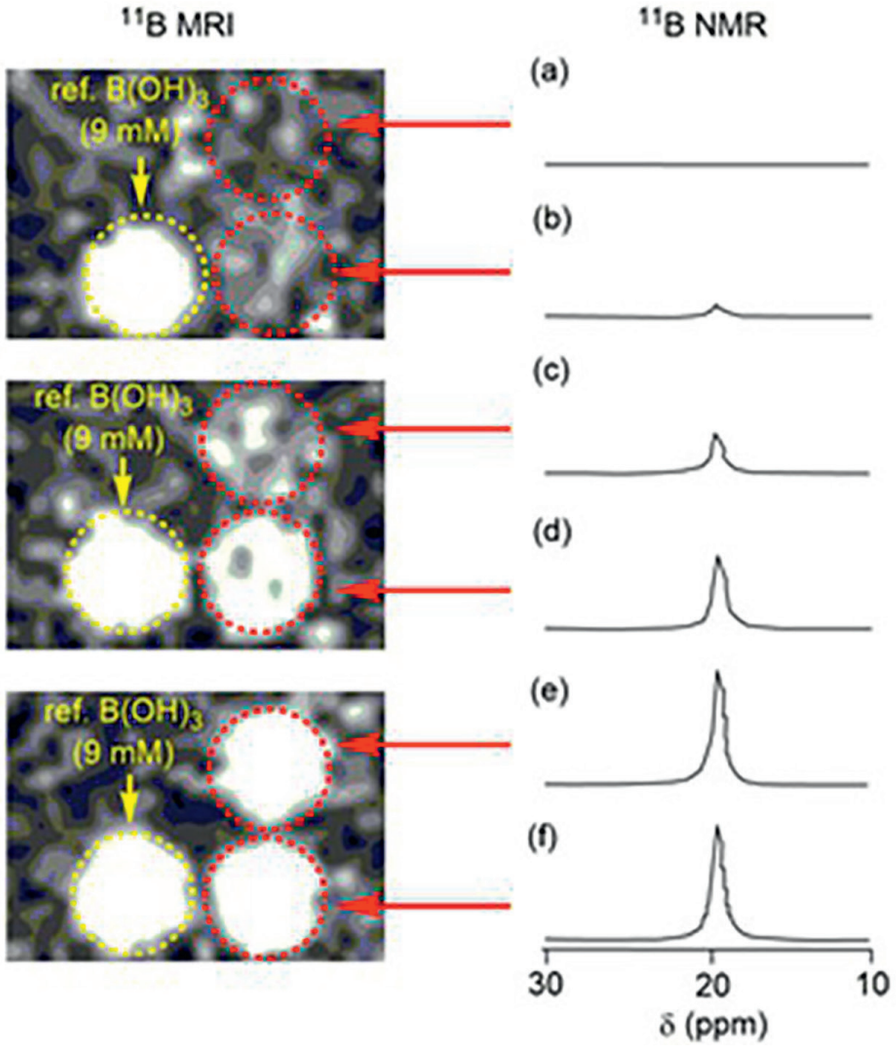

Figure 11.
^{11}B MRI and ^{11}B{^{1}H} NMR (128 MHz) spectra of **16** *(L^5) (2 mM) in DMSO/0.5 M HEPES buffer (pH 7)/D$_2$O (5:4:1, 0.5 mL in total) after incubation with various concentrations (0 (a), 0.02 (b), 0.1 (c), 0.2 (d), 1 (e), 2 mM (f)) of Cu^{2+} at 37 °C for 8 h (A 2.5% solution of BF$_3$·Et$_2$O in CDCl$_3$ was used as the external reference). ^{11}B NMR images were acquired by a two dimensional ultra-short echo time sequence (UTE2D) with BF1 values ≈ 128.392 MHz, TE = 199 μsec and TR = 30 msec.*

NMR signals of B(OH)$_3$ were successfully observed, and the signal intensities were increased in a dose-dependent manner due to the Cu^{2+}-promoted decomposition of **16** (L^5), as shown in **Figure 11**.

3. Design and synthesis of boron-containing agents for boron neutron capture therapy (BNCT)

3.1 General

As described in the Introduction, BNCT is one of the powerful cancer treatment methods utilizing two heavy particles, ^{4}He and ^{7}Li, which are produced from ^{10}B by a neutron capture reaction [^{10}B (n, α)^{7}Li] and induce the damage of biomolecules such as DNA, RNA, and so on within a short range of 5–9 μm [4–8]. For this BNCT to be achieved, the development of cancer-specific ^{10}B carriers is urgently needed. To date,

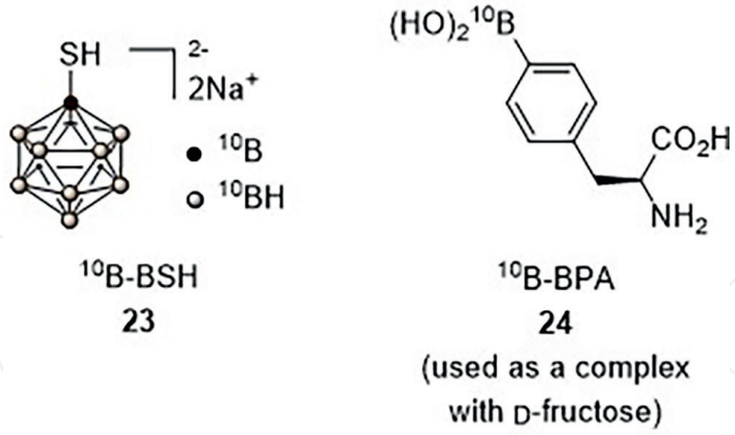

Figure 12.
Structures of representative BNCT agents.

only two boron compounds, namely disodium mercaptoundecahydrododecaborate (BSH) **23** and L-4-boronophenylalanine (BPA) **24** (used as a complex with D-fructose), have been approved for use as BNCT agents in clinical settings (**Figure 12**) [31, 32], but they are not sufficiently effective for the treatment of various tumor types. Because more selective and more efficient BNCT agents are required, the design and synthesis of new boron carriers based on sugar and macrocyclic polyamine scaffolds were conducted.

3.2 Design and synthesis of boron-containing sugars for BNCT

Sulfoquinovosyl acylglycerol (SQAG) **25** was isolated from sea algae and characterized by Sakaguchi et al., and **25** and its derivative sulfoquinovosyl acylpropanediol (SQAP) **26** were reported to be accumulated in cancer cells and exhibit weak toxicity against normal cells (**Figure 13a**) [33]. Because the modification of the long alkyl

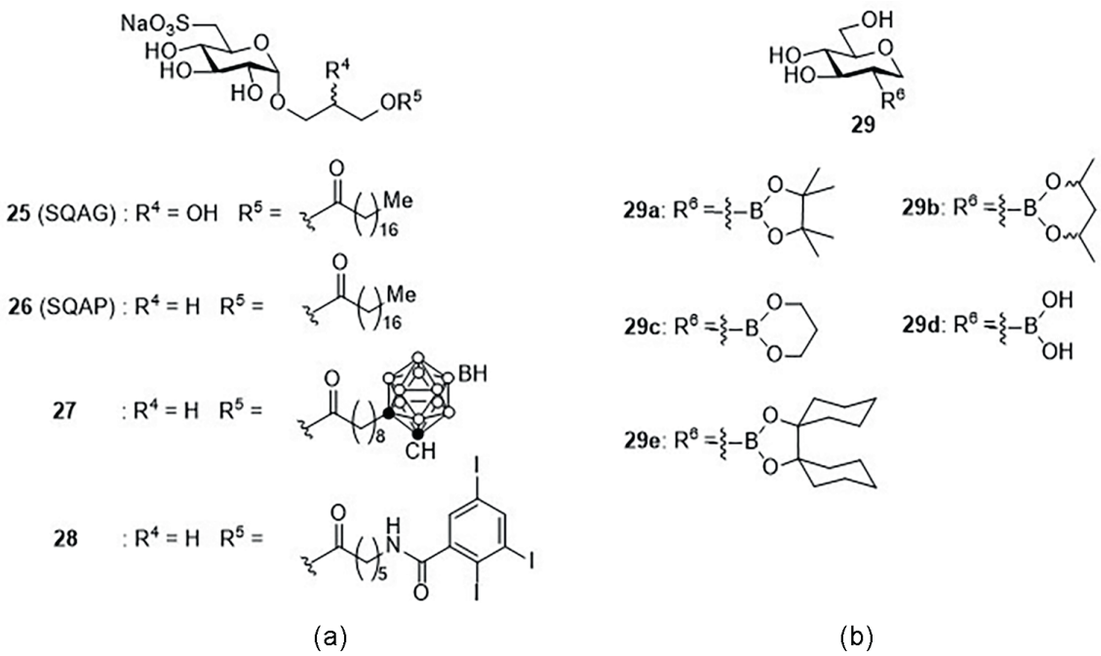

Figure 13.
Structures of (a) SQAG and SQAP derivatives and (b) 2-boryl-1,2-dideoxy-D-glucose derivatives.

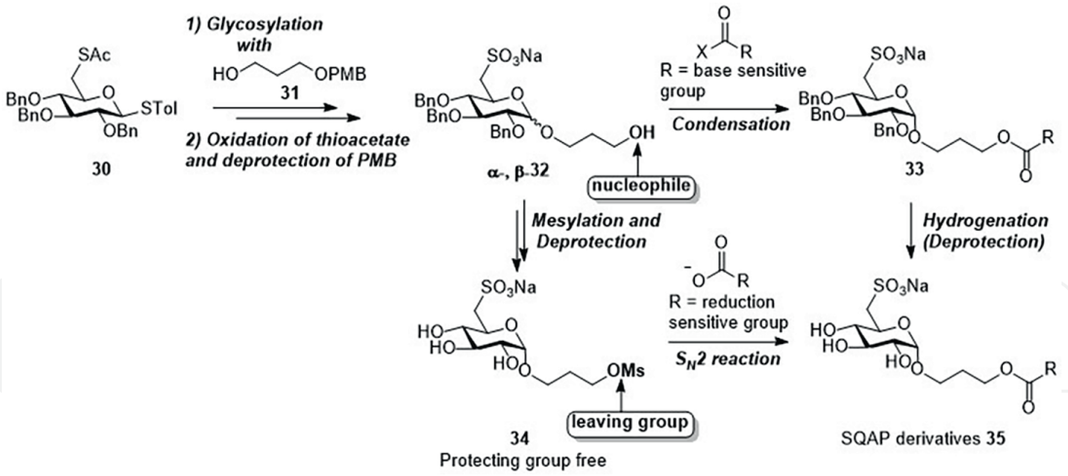

Figure 14.
The synthetic route of SQAP derivatives developed by Aoki et al.

chain of SQAG has negligible effect on its biological activity, the design and synthesis of SQAP derivatives **27** and **28** containing a boron cluster unit and iodine atoms as BNCT agents and imaging agents for X-ray computed tomography (CT) were conducted [34, 35].

The synthesis route for preparing SQAG analogues **27** and **28** is presented in **Figure 14**. The intermediate **32** was obtained by the α selective glycosylation of **30** with **31** in CH_2Cl_2/*tert*-butyl methyl ether (1/3), followed by the oxidation of thioacetate and the deprotection of *p*-methoxybenzyl (PMB) group. The condensation of **32** with a long chain fatty acid unit and subsequent deprotection of the benzyl groups could give the desired product **35**, which would be ideal for the synthesis of SQAP analogues containing base-sensitive functional groups such as carborane. Furthermore, the conversion of a nucleophile (-OH) of **32** to a leaving group (-OMs) enables the introduction of various acyl moieties by S_N2 reaction to give **35**, which corresponds to **27** and **28**. This novel synthesis route, as presented in **Figure 14**, would be useful for preparing a wide variety of SQAP derivatives.

The design and synthesis of 2-boryl-1,2-dideoxy-D-glucose derivatives **29a**–**e** were also carried out (**Figure 13b**) [36]. It is well known that cancer cells exhibit high glucose consumption and upregulation of glucose transporters (GLUTs) for rapid growth and proliferation, a process that is known as the Warburg effect [37]. It was also reported that hydrogen bonding interactions between the hydroxy groups of D-glucose and amino acid residues of GLUT trigger the intracellular uptake of glucose, and that the modification of D-glucose with bulky moieties at the C2 and C6 positions is tolerated [38]. In clinical applications, for instance, the D-glucose analogue, 2-deoxy-2-[^{18}F]fluoro-D-glucose, has been used for the diagnosis of cancer by means of positron emission tomography (PET) based on the aforementioned issues [39].

We therefore performed the regio- and stereoselective hydroboration of D-glucal **36** at the C1-C2 double bond, esterification with a diol, and deprotection of the hydroxy groups to provide **29a**–**e** via the intermediate **37** (**Figure 15**). Although hydroboration is one of traditional methods for the conversion of alkenes into alcohols such as **38** after the treatment of a boryl intermediate such as **37** with H_2O_2/NaOH, **37** was directly converted into **29**. Further investigations of their biological activity indicated that these sugar derivatives exhibit the moderate intracellular uptake against cancer cell lines through GLUT1, while their BNCT activity was not satisfying.

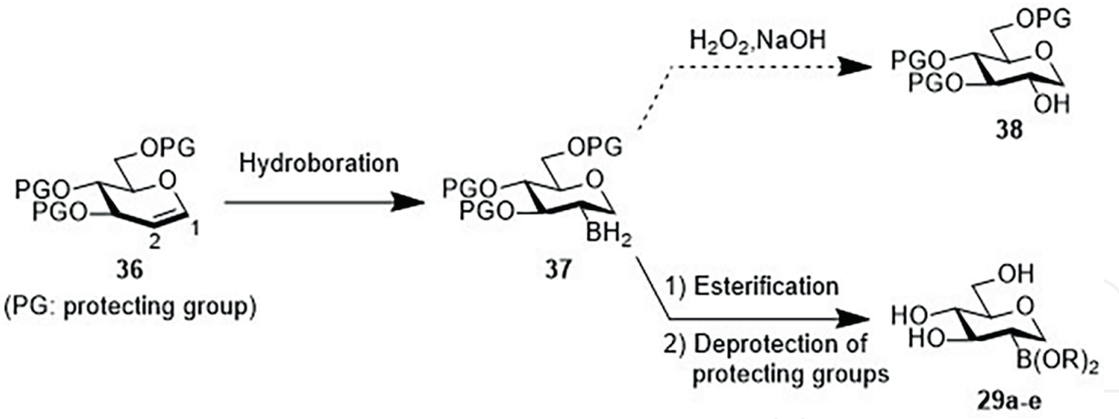

Figure 15.
Synthesis of 2-boryl-1,2-dideoxy-D-glucose derivatives **29a–e** *via the hydroboration of the protected D-glucal* **36**.

3.3 Design and synthesis of boron-containing macrocyclic polyamines for BNCT

It is known that natural polyamines play multiple roles in cellular functions, including gene expression and the stabilization of chromatin structure, and that the activated polyamine transport system and biosynthesis in cancer cells are related to the increase in polyamine concentrations and proliferation activity [40, 41]. Therefore, it is expected that polyamines would be desirable scaffolds for cancer selective and DNA-targeting boron delivery agents [42, 43].

Kimura and coworkers reported that Zn^{2+}–cyclen complexes **39** selectively recognize thymidine (dT) units in DNA to form a stable complex **40** in aqueous solution at neutral

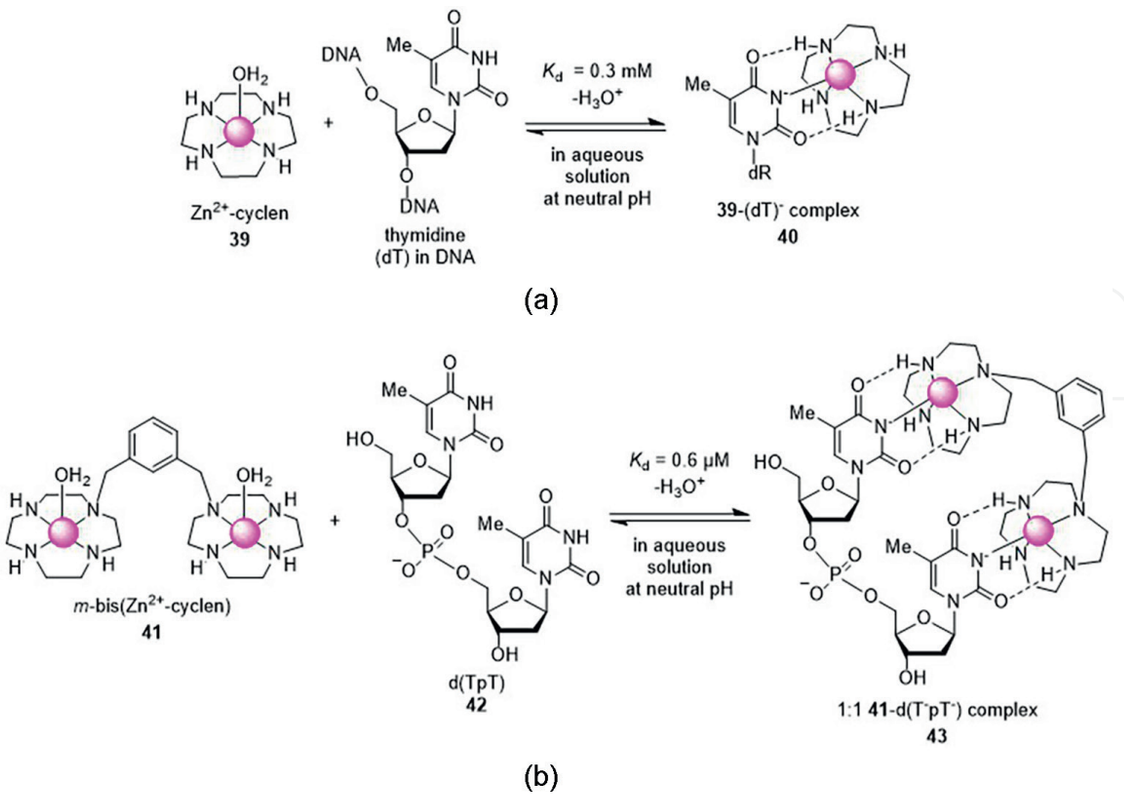

Figure 16.
Complexation of (a) Zn^{2+}–cyclen **39** *with the deprotonated form of thymidine (dT^-) and (b) bis(Zn^{2+}–cyclen)* **41** *with d(T^-pT^-)* **42** *in aqueous solution at neutral pH.*

pH by coordination bonding between the deprotonated imide part of dT (dT^-) and Zn^{2+} and by hydrogen bonding between the NH of cyclen and the imide oxygens of dT^- (**Figure 16a**) [44–47]. In addition, the bis(Zn^{2+}–cyclen) complexes **41** strongly bind two adjacent thymidine (thymidyl(3′–5′)thymidine, d(TpT)) **42**, yielding a very stable 1:1 complex **43** (**Figure 16b**) [48–51]. The dissociation constants (K_d) were reported to be 0.3 mM for **40** (1:1 complex of dT^- with **39**) and 0.6 μM for **43** (1:1 complex of $d(T^-pT^-)$ with **41**), respectively, at physiological pH in aqueous solution [52–54].

In this context, we designed and synthesized some novel DNA-targeting BNCT agents containing macrocyclic polyamine scaffolds such as [9]aneN$_3$, [12]aneN$_4$, and [15]aneN$_5$ and their Zn^{2+} complexes, which contain phenylboronic acid units, as shown in **Figures 17** and **18** [55, 56]. It was assumed that these boron-containing macrocyclic polyamine monomers **44–49** (L^6–L^{12}) and their Zn^{2+} complexes **50–52** (ZnL^6–ZnL^{12}) would be efficiently transferred into cancer cells and that thermal neutron irradiation would induce effective DNA damage in cancer cells due the ^{10}B atoms being located in close proximity to DNA molecules (**Figure 17**). We also expected that the interaction of homo- and heterodimer of macrocyclic polyamines **53–62** (L^{13}–L^{22}) and their corresponding monozinc(II) complexes **63–68** (ZnL^{13}–ZnL^{21}) and dizinc(II) complexes **69–78** (Zn_2L^{13}–Zn_2L^{22}) with DNA would be stronger than that of monomeric polyamines, resulting in efficient DNA damage upon thermal neutron irradiation (**Figure 18**). These mono- and

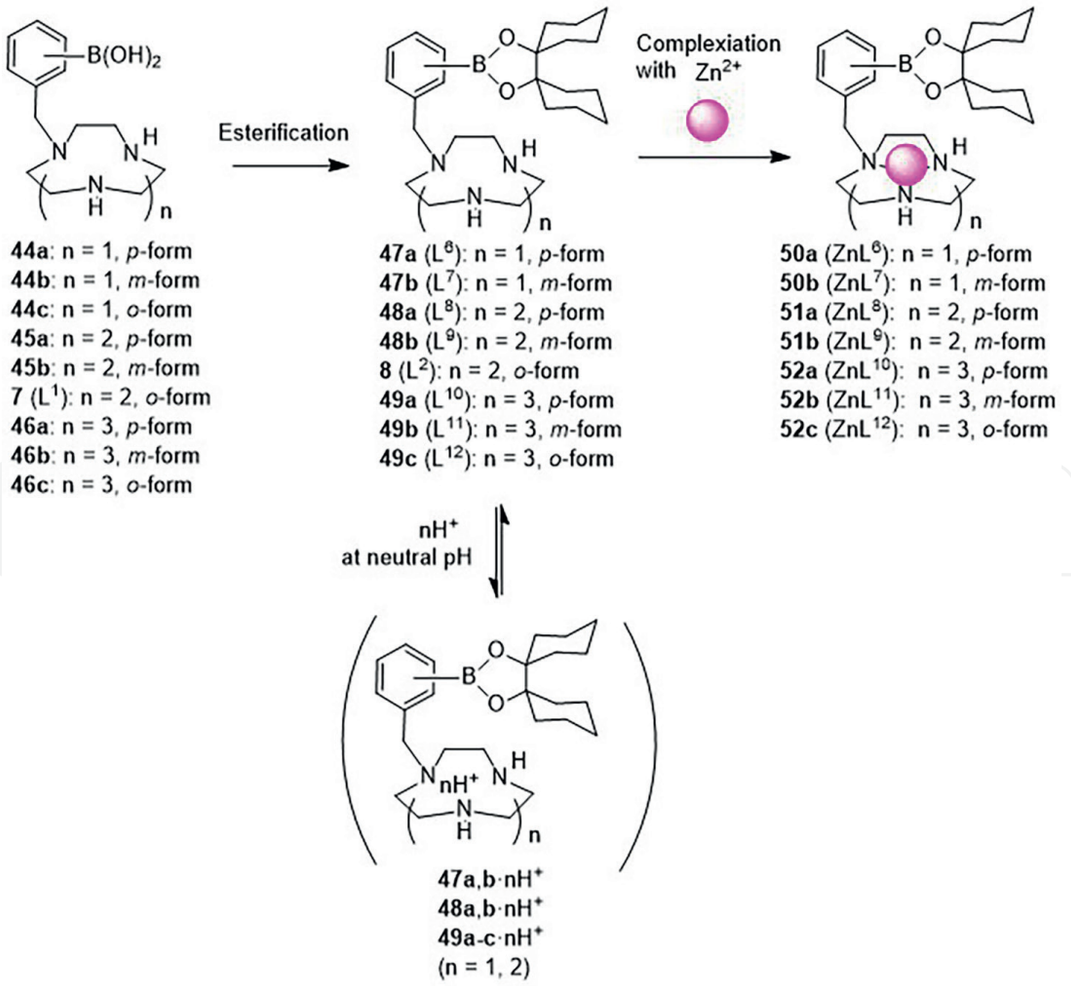

Figure 17.
Structures of B-containing macrocyclic polyamine monomers and their Zn^{2+} complexes.

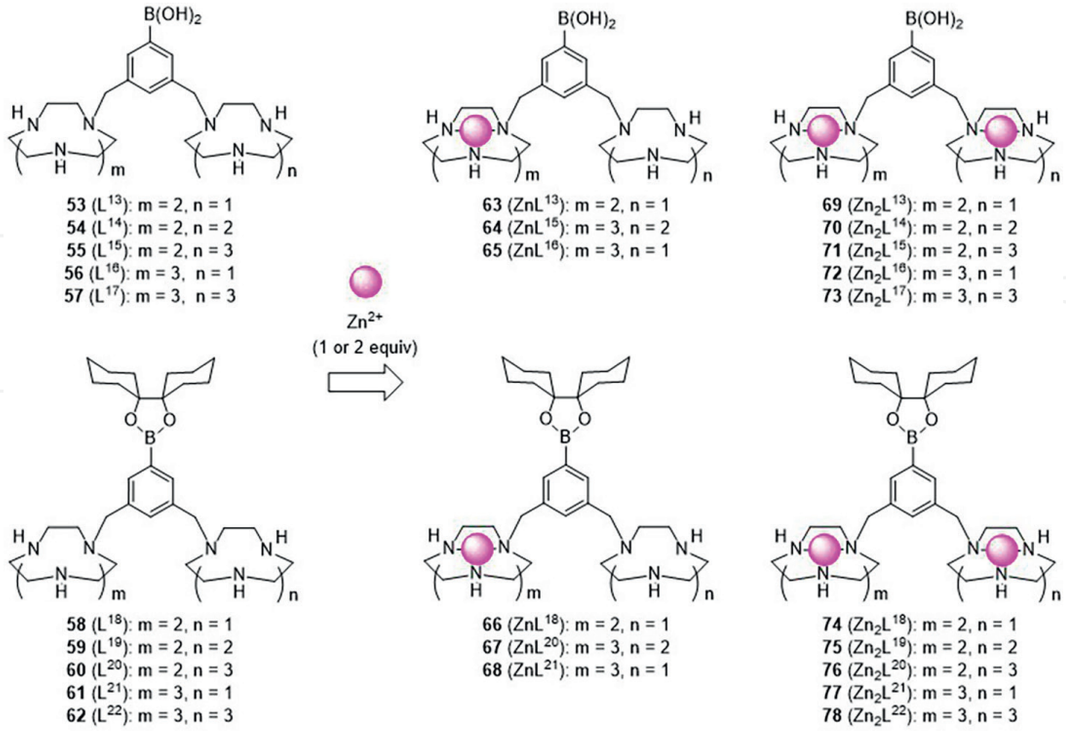

Figure 18.
Structures of B-containing macrocyclic polyamine dimers **53–62** *(L^{13}–L^{22}) and their Zn^{2+} complexes* **63–78** *(ZnL^{13}–ZnL^{21} and Zn_2L^{13}–Zn_2L^{22}).*

dimeric macrocyclic polyamines were first prepared with boron in a natural abundance ratio ($^{10}B/^{11}B$ = 19.9/80.1) to evaluate their cytotoxicity and intracellular uptake in several cancer cell lines, and some of the promising compounds were synthesized in the corresponding ^{10}B-enriched forms for the BNCT experiments. It should also be noted that these compounds possess macrocyclic polyamine units at the *m*- or *p*-position, but not at the *o*-position, of the C–B bonds to avoid the C–B hydrolysis upon metal complexation, as described in **Figures 2** and **3**.

The results of biological studies suggested that the boron-containing macrocyclic polyamine monomers **47b** (L^7), **48b** (L^9), and **49a** (L^{10}) have a weak cytotoxicity against normal cells and are efficiently transferred into cancer cells such as A549 and HeLa S3 cells, possibly via a polyamine transport system. In addition, it was found that ditopic macrocyclic polyamines possess much less cytotoxicity than that of the monomers and moderate uptake activity into cancer cells. Therefore, some of the more promising compounds were selected and their ^{10}B-enriched forms (>99% of ^{10}B) were prepared for BNCT experiments.

In vitro neutron irradiation experiments using A549 cells in the presence of the ^{10}B-enriched **^{10}B-47b** (L^7), **^{10}B-48b** (L^9), and **^{10}B-49a** (L^{10}) were performed at the Institute for Integrated Radiation and Nuclear Science, Kyoto University, and the BNCT effect of these drugs was evaluated by colony formation assays. It was found that **^{10}B-47b** (L^7), **^{10}B-48b** (L^9), and **^{10}B-49a** (L^{10}) showed higher cytotoxic effects than ^{10}B-BSH **23** and ^{10}B-BPA **24** and that the BNCT effect of ^{10}B-enriched dimers is nearly the same as ^{10}B-BPA (**Figure 19**). The BNCT effect of **^{10}B-47b** (L^7) and **^{10}B-50b** (ZnL^7) is almost identical and that of **^{10}B-50b** (ZnL^7) is even better, although the intracellular uptake of the Zn^{2+} complexes is generally lower than that of the corresponding Zn^{2+}-free ligands. It is possibly due to weak complexation of the 9-membered ring of **^{10}B-47b** (L^7) with Zn^{2+}. In addition, 12- and 15-membered macrocycles

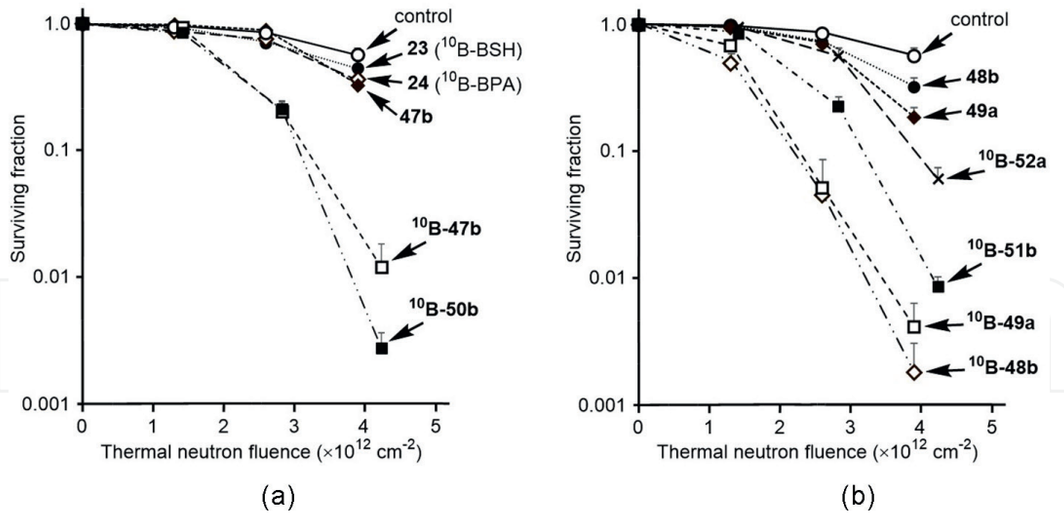

Figure 19.
BNCT effect of macrocyclic polyamine monomers **23**, **24**, **47b**, **^{10}B-47b**, **48b**, **^{10}B-48b**, **49a**, **^{10}B-49a**, **^{10}B-50b**, **^{10}B-51b**, *and* **^{10}B-52a** *(30 μM) against A549 cells was examined by a colony formation assay: (a) control (in the absence of a boron compound) (○),* **23** *(•),* **24** *(◇),* **47b** *(◆),* **^{10}B-47b** *(□), and* **^{10}B-50b** *(■). (b) Control (○),* **48b** *(•),* **^{10}B-48b** *(◇),* **49a** *(◆), and* **^{10}B-49a** *(□), and* **^{10}B-51b** *(■), and* **^{10}B-52a** *(×). After treatment with the boron compound for 24 h, the cells were irradiated with thermal neutrons for 0, 15, 30, and 45 min and then incubated without neutron irradiation for 7 days.*

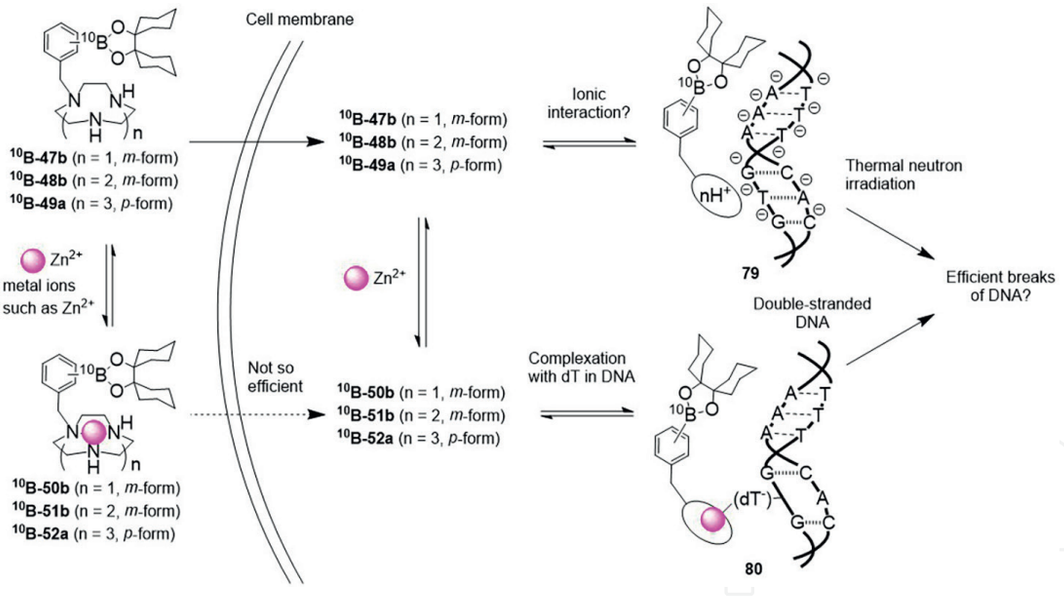

Figure 20.
Proposed scheme for BNCT effect of **^{10}B-47b**, **^{10}B-48b**, **^{10}B-49a** *and their Zn^{2+} complexes.*

^{10}B-48b and **^{10}B-49a** effectively inhibited the proliferation of cancer cells upon irradiation with thermal neutrons, while their intracellular uptake was lower than that of the [9]aneN_3-type **47b**.

According to the results of biological evaluations and DNA interaction studies using double-stranded calf-thymus DNA, it was concluded that metal-free monomers would be efficiently taken up by cancer cells and then form complexes with intracellular Zn^{2+}. Both the cationic metal-free macrocycles and their Zn^{2+} complexes would bind to DNA via electrostatic interactions between cationic macrocyclic polyamine moieties and anionic double-stranded DNA (**79** in **Figure 20**), or via the selective

recognition of Zn^{2+}-complexes such as **^{10}B-51b** with dT^- units in DNA as depicted in **Figure 16** (and **80** in **Figure 20**), resulting in effective DNA damage upon thermal neutron irradiation (**Figure 20**). These findings suggest that ^{10}B delivery agents equipped with monomeric [12]aneN_4- and [15]aneN_5-type macrocycles are preferable for use in BNCT.

4. Conclusion

In this review, we summarize the current state of knowledge regarding the design and synthesis of ^{10}B and/or ^{11}B containing agents for biomedical applications such as ^{11}B NMR probes and BNCT agents. We developed the d-block metal ion probes based on changes in ^{11}B NMR signals due to the hydrolysis of C–B bond in **7** (L^1) and **8** (L^2) and the decomposition of *o*-carborane moieties in derivatives such as **14** and **16** (L^5) upon complexation with metal ions in aqueous solution at physiological pH. Some novel BNCT agents based on sugar and macrocyclic polyamine scaffolds were also designed and synthesized. The findings indicate that ^{10}B-enriched monomeric macrocyclic polyamines **^{10}B-48b** (L^9) and **^{10}B-49a** (L^{10}) exhibit potent BNCT activity upon thermal neutron irradiation, possibly due to interaction with DNA, resulting in the efficient damage of DNA molecules that are in close proximity to the boron compounds.

We believe that this review provides useful information for the future design and synthesis of novel boron-containing compounds and their applications for the treatment and diagnosis of cancer and other diseases, as well as in related research fields.

Acknowledgements

We wish to thank our collaborators and coworkers for their contributions to work described in this review. We appreciate Dr. Motoo Shiro (Rigaku Co. Ltd.), Prof. Reiko Kuroda (Chubu University), and Dr. Yasuyuki Yamada (Nagoya University) for their great assistance and helpful discussion. Financial supports from the Ministry of Education, Culture, Sports, Science and Technology (MEXT) of Japan, the Uehara Memorial Foundation, the Tokyo Ohka Foundation for the Promotion of Science and Technology, Kanagawa, Japan, the Tokyo Biochemical Research Foundation, Tokyo, Japan, Japan Society for the Promotion of Science (JSPS), and Tokyo University of Science are gratefully acknowledged.

Conflicts of interest

The authors declare no conflict of interest.

Author details

Shin Aoki[1,2,3]*, Hiroki Ueda[1,4], Tomohiro Tanaka[1], Taiki Itoh[1], Minoru Suzuki[4] and Yoshinori Sakurai[4]

1 Faculty of Pharmaceutical Sciences, Tokyo University of Science, Noda, Chiba, Japan

2 Research Institute for Science and Technology, Tokyo University of Science, Noda, Chiba, Japan

3 Research Institute for Biomedical Sciences, Tokyo University of Science, Noda, Chiba, Japan

4 Institute for Integrated Radiation and Nuclear Science, Kyoto University, Osaka, Japan

*Address all correspondence to: shinaoki@rs.tus.ac.jp

References

[1] Heřmánek S. ^{11}B NMR spectra of boranes, main-group heteroboranes, and substituted derivatives. factors influencing chemical shifts of skeletal atoms. Chemical Reviews. 1992;**92**:325-362

[2] Rinard PM. Neutron interactions with matter. In: Reilly D, Ensslin N, Smith H, Kreiner S, editors. Passive Nondestructive Assay of Nuclear Materials. Washington: Nuclear Regulatory Commission; 1991. pp. 357-377

[3] Morin C. The chemistry of boron analogues of biomolecules. Tetrahedron. 1994;**50**:12521-12569. DOI: 10.1016/S0040-4020(01)89389-3

[4] Locher GL. Biological effects and therapeutic possibilities of neutrons. The American Journal of Roentgenology and Radium Therapy. 1936;**36**:1-13

[5] Soloway AH, Tjarks W, Barnum BA, Rong FG, Barth RF, Codogni IM, et al. The chemistry of neutron capture therapy. Chemical Reviews. 1998;**98**:1515-1562. DOI: 10.1021/cr941195u

[6] Salt C, Lennox AJ, Takagaki M, Maguire JA, Hosmane NS. Boron and gadolinium neutron capture therapy. Russian Chemical Bulletin. 2004;**53**:1871-1888. DOI: 10.1007/s11172-005-0045-6

[7] Barth RF, Coderre JA, Vicente MGH, Blue TE. Boron neutron capture therapy of cancer: Current status and future prospects. Clinical Cancer Research. 2005;**11**:3987-4002

[8] Suzuki M. Boron neutron capture therapy (BNCT): A unique role in radiotherapy with a view to entering the accelerator-based BNCT era. International Journal of Clinical Oncology. 2020;**25**:43-50. DOI: 10.1007/s10147-019-01480-4

[9] Dai Q, Yang Q, Bao X, Chen J, Han M, Wei Q. The development of boron analysis and imaging in boron neutron capture therapy (BNCT). Molecular Pharmaceutics. 2022;**19**:363-377. DOI: 10.1021/acs.molpharmaceut.1c00810

[10] McRae R, Bagchi P, Sumalekshmy S, Fahrni CJ. In situ imaging of metals in cells and tissues. Chemical Reviews. 2009;**109**:4780-4827. DOI: 10.1021/cr900223a

[11] Que EL, Domaille DW, Chang CJ. Metals in neurobiology: Probing their chemistry and biology with molecular imaging. Chemical Reviews. 2008;**108**:1517-1549. DOI: 10.1021/cr078203u

[12] Zhu H, Fan J, Wang B, Peng X. Fluorescent, MRI, and colorimetric chemical sensors for the first-row d-block metal ions. Chemical Society Reviews. 2015;**44**:4337-4366. DOI: 10.1039/c4cs00285g

[13] Hingorani DV, Bernstein AS, Pagel MD. A review of responsive MRI contrast agents: 2005-2014. Contrast Media & Molecular Imaging. 2015;**10**:245-265. DOI: 10.1002/cmmi.1629

[14] Caravan P, Ellison JJ, McMurry TJ, Lauffer RB. Gadlinium(III) chelates as MRI contrast agents: Structure, dynamics, and applications. Chemical Reviews. 1999;**99**:2293-2352

[15] Xu Z, Liu C, Zhao S, Chen S, Zhao Y. Molecular sensors for NMR-based detection. Chemical Reviews.

2019;**119**:195-230. DOI: 10.1021/acs.chemrev.8b00202

[16] Kodama M, Kimura E. Equilibria and kinetics of complex formation between zinc(II), lead(II), andcadmium(II), and 12-, 13-, 14-, and 15-memberd macrocyclic tetraamines. Journal of the Chemical Society Dalton Transactions. 1977:2269-2276. DOI: 10.1039/DT9770002269

[17] Kodama M, Kimura E. Equilibria of Complex formation between several bivalent metal ions and macrocyclic tri- and penta-amines. Journal of the Chemical Society Dalton Transactions. 1978:1081-1085. DOI: 10.1039/DT9780001081

[18] Kimura E. Macrocyclic polyamines with intelligent functions. Tetrahedron. 1992;**48**:6175-6217. DOI: 10.1016/S0040-4020(01)88212-0

[19] Kimura E. Model studies for molecular recognition of carbonic anhydrase and carboxypeptidase. Accounts of Chemical Research. 2001;**34**:171-179. DOI: 10.1021/ar000001w

[20] Itoh S, Sonoike S, Kitamura M, Aoki S. Design and synthesis of chiral Zn^{2+} complexes mimicking natural aldolases for catalytic C–C bond forming reactions in aqueous solution. International Journal of Molecular Sciences. 2014;**15**:2087-2118. DOI: 10.3390/ijms15022087

[21] Aoki S, Zulkefeli M, Kitamura M, Hisamatsu Y. Supramolecular host and catalysts formed by the synergistic molecular assembly of multinuclear zinc(II) complexes in aqueous solution. In: Nabeshima T, editor. Synergy in Supramolecular Chemistry. Boca Raton: CRC; 2015. pp. 33-56. DOI: 10.1201/b17940

[22] Kimura E, Koike T, Aoki S. Evolution of Zn^{II}–macrocyclic polyamines to biological probes and supramolecular assembly. In: Izatt RM, editor. Macrocyclic and Supramolecular Chemistry: How Izatt-Christensen Award Winners Shaped the Field. Hoboken: John Wiley & Sons; 2016. pp. 417-445. DOI: 10.1002/9781119053859.ch21

[23] Aoki S, Rahman AB, Hisamatsu Y, Miyazawa Y, Zulkefeli M, Saga Y, et al. Development of metallosupramolecular phosphatases based on the combinatorial self-assembly of metal complexes and organic building blocks for the catalytic hydrolysis of phosphate monoesters. Result in Chemistry. 2021;**3**:100133. DOI: 10.1016/j.rechem.2021.100133

[24] Bendel P. Biomedical applications of ^{10}B and ^{11}B NMR. NMR in Biomedicine. 2005;**18**:74-82. DOI: 10.1002/nbm.886

[25] Bendel P, Margalit R, Koudinova N, Salomon Y. Noninvasive quantitative in vivo mapping and metabolism of boronophenylalanine (BPA) by nuclear magnetic resonance (NMR) spectroscopy and imaging. Radiation Research. 2005;**164**:680-687. DOI: 10.1667/RR3450.1

[26] Kitamura M, Suzuki T, Abe R, Ueno T, Aoki S. ^{11}B NMR Sensing of d-block metal ions in vitro and in cells based on a carbon–boron bond cleavage of phenylboronic acid-pendant cyclen (cyclen = 1,4,7,10-tetraazacyclododecane). Inorganic Chemistry. 2011;**50**:11568-11580. DOI: 10.1021/ic201507q

[27] Ohshima R, Kitamura M, Morita A, Shiro M, Yamada Y, Ikekita M, et al. Design and synthesis of fluorescent probe for Zn^{2+}, 5,7-bis(*N*,*N*-dimethylaminosulfonyl)-8-hydroxyquinoline-pendant

1,4,7,10-tetraazacyclododecane and Zn^{2+}-dependent hydrolytic and Zn^{2+}-independent photochemical reactivation of its benzenesulfonyl-caged derivatives. Inorganic Chemistry. 2010;**49**:888-899. DOI: 10.1021/ic901279t

[28] Hawthorne MF. The role of chemistry in the development of boron neutron capture therapy of cancer. Angewandte Chemie, International Edition. 1993;**32**:950-984. DOI: 10.1002/anie.199309501

[29] Tanaka T, Nishiura Y, Araki R, Saido T, Abe R, Aoki S. ^{11}B NMR probes of copper(II): Finding and implications of the Cu^{2+}-promoted decomposition of *ortho*-carborane derivatives. European Journal of Inorganic Chemistry. 2016;**2016**(12):1819-1834. DOI: 10.1002/ejic.201600117

[30] Tanaka T, Araki R, Saido T, Abe R, Aoki S. ^{11}B NMR/MRI sensing of copper(II) ions in vitro by the decomposition of a hybrid compound of a *nido-o*-carborane and a metal chelator. European Journal of Inorganic Chemistry. 2016;**2016**(20):3330-3337. DOI: 10.1002/ejic.201600346

[31] Cerecetto H, Couto M. Medicinal chemistry of boron-bearing compounds for BNCT-glioma treatment: Current challenges and perspectives. In: Omerhodžić I, Arnautović K, editors. Glioma – Contemporary Diagnostic and Therapeutic Approaches. London, UK: IntechOpen; 2018. pp. 205-230. DOI: 10.5772/intechopen.76369

[32] Hu K, Yang Z, Zhang L, Xie L, Wang L, Xu H, et al. Boron agents for neutron capture therapy. Coordination Chemistry Reviews. 2020;**405**:213139. DOI: 10.1016/j.ccr.2019.213139

[33] Ohta K, Mizushina Y, Yamazaki T, Hanashima S, Sugawara F, Sakaguchi K. Specific interaction between an oligosaccharide on the tumor cell surface and the novel antitumor agents, sulfoquinovosylacylglycerols. Biochemical and Biophysical Research Communications. 2001;**288**:893-900. DOI: 10.1006/bbrc.2001.5852

[34] Brahmi MM, Portmann C, D'Ambrosio D, Woods TM, Banfi D, Reichenbach P, et al. Telomerase inhibitors from cyanobacteria: Isolation and synthesis of sulfoquinovosyl diacylglycerols from Microcystis aeruginosa PCC 7806. Chemistry--A European Journal. 2013;**19**:4596-4601. DOI: 10.1002/chem.201203296

[35] Tanaka T, Sawamoto Y, Aoki S. Concise and versatile synthesis of sulfoquinovosyl acyl glycerol derivatives for biological applications. Chemical & Pharmaceutical Bulletin. 2017;**65**:566-572. DOI: 10.1248/cpb.c17-00135

[36] Itoh T, Tamura K, Ueda H, Tanaka T, Satoh K, Kuroda R, et al. Design and synthesis of boron containing monosaccharides by the hydroboration of D-glucal for use in boron neutron capture therapy (BNCT). Bioorganic & Medicinal Chemistry. 2018;**26**:5922-5933. DOI: 10.1016/j.bmc.2018.10.041

[37] Heiden MGV, Cantley LC, Thompson CB. Understanding the Warburg effect: The metabolic requirements of cell proliferation. Science. 2009;**324**:1029-1033. DOI: 10.1126/science.1160809

[38] Calvaresi EC, Hergenrother PJ. Glucose conjugation for the specific targeting and treatment of cancer. Chemical Science. 2013;**4**:2319-2333. DOI: 10.1039/C3SC22205E

[39] Patching SG. Role of facilitative glucose transporter GLUT1 in [18F]FDG positron emission tomography (PET)

imaging of human diseases. Journal of Diagnostic Imaging in Therapy. 2015;**2**:30-102

[40] Nowotarski SL, Woster PM, Casero RA. Polyamines and cancer: Implications for chemoprevention and chemotherapy. Expert Reviews in Molecular Medicine. 2013;**15**:e3. DOI: 10.1017/erm.2013.3

[41] Murray-Stewart TR, Woster PM, Casero RA. Targeting polyamine metabolism for cancer therapy and prevention. The Biochemical Journal. 2016;**473**:2937-2953. DOI: 10.1042/BCJ20160383

[42] Hosmane NS, Maguire JA, Zhu Y, Takagaki M. Boron and Gadolinium Neutron Capture Therapy for Cancer Treatment. Singapore: World Scientific Publishing; 2012. p. 272

[43] Zhuo JC, Cai J, Soloway AH, Barth RF, Adams DM, Ji W, et al. Synthesis and biological evaluation of boron-containing polyamines as potential agents for neutron capture therapy of brain tumors. Journal of Medicinal Chemistry. 1999;**42**:1282-1292. DOI: 10.1021/jm960787x

[44] Shionoya M, Kimura E, Shiro M. A new ternary zinc(II) complex with [12] aneN_4 (= 1,4,7,10-tetraazacyclododecane) and AZT (= 3'-azido-3'-deoxythymine). highly selective recognition of thymidine and its related nucleosides by a zinc(II) macrocyclic tetraamine complex with novel complementary associations. Journal of the American Chemical Society. 1993;**115**:6730-6737

[45] Kimura E, Ikeda T, Aoki S, Shionoya M. Macrocylic zinc(II) complexes for selective recognition of nucleobases in single- and double-stranded polynucleotides. Journal of Biological Inorganic Chemistry. 1998;**3**:259-267. DOI: 10.1007/s007750050230

[46] Kikuta E, Murata M, Katsube N, Koike T, Kimura E. Novel recognition of thymine base in double-stranded DNA by zinc(II)–macrocyclic tetraamine complexes appended with aromatic groups. Journal of the American Chemical Society. 1999;**121**:5426-5436. DOI: 10.1021/ja983884j

[47] Kimura E, Kikuta E. Why zinc in zinc enzymes? From biological roles to DNA based-selective recognition. Journal of Biological Inorganic Chemistry. 2000;**5**:139-155. DOI: 10.1007/s007750050359

[48] Aoki S, Sugimura C, Kimura E. Efficient inhibition of photo[2 + 2] cycloaddition of thymidilyl(3′–5′) thymidine and promotion of photosplitting of the cis-syn- cyclobutane thymine dimer by dimeric zinc(II)–cyclen complexes containing *m*- and *p*-xylyl spacers. Journal of the American Chemical Society. 1998;**120**:10094-10102. DOI: 10.1021/ja981788c

[49] Kimura E, Kikuchi M, Kitamura H, Koike T. Selective and efficient recognition of thymidylylthymidine (TpT) by bis(Zn^{II}–cyclen) and thymidylylthymidylylthymidine (TpTpT) by tris(Zn^{II}–cyclen) at neutral pH in aqueous solution. Chemistry--A European Journal. 1999;**5**:3113-3123. DOI: 10.1002/(SICI)1521-3765(19991105)5:11<3113::AID-CHEM3113>3.0.CO;2-L

[50] Aoki S, Kimura E. Highly selective recognition of thymidine mono- and diphosphate nucleotides in aqueous solution by ditopic receptors zinc(II)–bis(cyclen) complexes (cyclen = 1,4,7,10-tetraazacyclododecane). Journal of the American Chemical Society. 2000;**122**:4542-4548. DOI: 10.1021/ja994537s

[51] Kikuta E, Aoki S, Kimura E. A new type of potent inhibitors of HIV-1 TAR RNA–Tat peptide binding by zinc(II)–macrocyclic tetraamine complexes. Journal of the American Chemical Society. 2001;**123**:7911-7912. DOI: 10.1021/ja0108335

[52] Kimura E, Kikuta E. Macrocyclic zinc(II) complexes for selective recognition of nucleobases in single- and double-stranded polynucleotides. Progress in Reaction Kinetics and Mechanism. 2000;**25**:1-64. DOI: 10.3184/007967400103165119

[53] Aoki S, Kimura E. Zinc–nucleic acid interaction. Chemical Reviews. 2004;**104**:769-788. DOI: 10.1021/cr020617u

[54] Kimura E. Evolution of macrocyclic polyamines from molecular science to supramolecular science. Bulletin of Japan Society of Coordination Chemistry. 2012;**59**:26-47. DOI: 10.4019/bjscc.59.26

[55] Ueda H, Suzuki M, Kuroda R, Tanaka T, Aoki S. Design, synthesis, and biological evaluation of boron-containing macrocyclic polyamines and their zinc(II) complexes for boron neutron capture therapy. Journal of Medicinal Chemistry. 2021;**64**:8523-8544. DOI: 10.1021/acs.jmedchem.1c00445

[56] Ueda H, Suzuki M, Sakurai Y, Tanaka T, Aoki S. Design, synthesis and biological evaluation of boron-containing macrocyclic polyamine dimers and their zinc(II) complexes for boron neutron capture therapy. European Journal of Inorganic Chemistry. 2022;**2022**:e202100949. DOI: 10.1002/ejic.202100949